

DIAGNOSTIC VALUE OF LYMPH NODE CALCIFICATION IN THYROID CANCER

Andrii Kurochkin¹

Roman Moskalenko²

DOI: <https://doi.org/10.30525/978-9934-26-195-4-23>

Abstract. The role of pathological biomineralization (PBM) as a prognostic and diagnostic marker in thyroid cancer is continuously debated among investigators. Detection of pathological biomineralization in the lymph nodes of the neck is an alarming signal for clinicians. Typically, a lymph node with signs of calcification is a symptom of papillary thyroid cancer. The lymph node contains such a form of calcification as psammoma bodies in such cases. Psammoma bodies of relatively large size (more than 200 μm) can be detected by ultrasound. Our study aims to study the crystal-chemical and phase characteristics of calcifications of metastatic lymph nodes in thyroid cancer to develop promising methods of early diagnosis. *Materials and methods.* Several complex research methods have been conducted for a deeper understanding of the pathological biomineralization of metastatic lymph nodes in thyroid cancer, such as macroscopic examination, ultrasound diagnostics, detection of strict lymph node, histological, histochemical, and electron microscopic (scanning electron microscopy, X-ray diffraction, and transmission electron microscopy). Our study found that the main component of pathological biomineral deposits is calcium phosphate compounds. The Ca / P ratio corresponds to the characteristic features of hydroxyapatite. A significant proportion of β -tricalcium magnesium phosphate was also detected in some cases. The specific plate structure and the known phase and crystal-chemical composition of psammoma bodies can be the point of application of searches for their early detection using the latest diagnostic methods with high resolution. *Conclusion.* Our study demonstrated the significance of PBM in lymph nodes as a diagnostic symptom of papillary thyroid cancer patients. The presence and extent of PBM in the lymph nodes

¹ PhD student, Department of Oncology,
Sumy State University, Ukraine

² Doctor of Medical Sciences, Professor,
Department of Pathology, Sumy State University, Ukraine

should be considered a metastasis of papillary thyroid cancer. The study of the structure, physicochemical, phase composition of lymph node calcifications, and visualization features is promising given the possible practical application for early diagnosis of metastases of papillary thyroid cancer.

1. Introduction

Thyroid cancer (TC) is the most common endocrine malignancy, and its incidence has been increasing worldwide over the years [1]. Thyroid cancer classification into Differentiated Thyroid Cancer (DTC), Lowly Differentiated Thyroid Cancer (PDTC), and Undifferentiated Thyroid Cancer (UTC) according to the World Health Organization (WHO) (3). DTCs, including papillary thyroid cancer (PTC), follicular thyroid carcinoma (FTC), and Hurthle cell carcinoma (HCC), account for 95% of thyroid cancers and have a better prognosis than PDTC and ATC [2].

DTCs typically show sluggish behavior with a 10-year survival rate of approximately 90–95% [1; 2; 3]. Various clinical and pathological factors affect patient outcomes, such as old age, male gender, large tumor size, nodular or distant metastases [4].

The problem of thyroid disease is also relevant in Ukraine, especially after the Chernobyl accident. Statistical accounting of thyroid cancer in Ukraine began in 1989, when the incidence among men was 1.01 per 100 thousand population, among women – 3.54. These figures are growing every year. The total incidence of thyroid cancer in 2012 in Ukraine was 5.5 per 100 thousand population (among men – 2.2, and among women – 8.3), and in 2019 – 9.3 per 100 thousand. population (men – 3.8, women – 14.2). According to standardized indicators in 2019, the incidence in Ukraine exceeds the world by 26%, mortality – by 100% [5; 6].

Treatment of patients with differentiated thyroid cancer with clinically undetected metastases to regional lymph nodes is an unresolved problem of modern oncology. According to recent studies, the status of the regional lymphatic collector is not a prognostic factor in the survival of patients. Therefore, the search for reliable methods for diagnosing metastatic lymph nodes in thyroid time is one of the highest priorities. After morphological examination of the sentinel lymph node, selective lymph dissection helps achieve effective diagnostics. Diagnosis of sentinel lymph nodes (SLN) and study of their morphological status allow to obtain complete information

about the stage of thyroid cancer, plan further therapy and form a prognosis individually for each patient [7].

Clinicians used Isosulfan blue for imaging for SLN biopsy, which has many side effects: it stains adjacent tissues and adipose tissue, which interferes with the visualization of tissue structures and complicates histological examination. We previously conducted a study on the use of 1% toluidine blue, which showed an improvement in the quality of SLN biopsy [8].

One of the clinical and morphological features of the manifestation of thyroid tumors is calcification [9]. However, despite the relatively high detection frequency, the predictive and diagnostic values are not yet fully understood. Calcifications appear in the earliest malignant tumor development stages in the form of nanocrystalline objects [10; 11].

Ultrasound examination of the thyroid gland is an affordable and effective method for diagnosing the pathology of this organ. Pathological biomineralization in the lymph nodes is an alarming signal about the risk of detecting a malignant tumor [12]. The overall survival rate of patients with thyroid cancer depends on many predictors, including pathological biomineralization [13].

This characteristic mineralization is manifested in the development of so called psammoma bodies (PBs), which are round-shaped mineral formations with concentric layers. PBs are distinct from the micro-spheruliths, which are also circular but have no lamellar structure [13, 14]. To date, the clinical importance of the PBs as well as the molecular mechanisms of their formation and the causes of mineralization remain unclear [14].

Calcifications > 1 mm with posterior acoustic shadow are macrocalcifications, and although there are some different classifications for the types of macrocalcifications [15], the most commonly found terms are “egg-shell, annular or rim-like peripheral calcification” and “coarse dense calcifications” [16]. Regardless of size, all the aforementioned types of calcification represent forms of so-called dystrophic calcification (DC), since one is dealing with calcification occurring in degenerated or necrotic tissue.

On the basis of histological features of thyroid carcinoma, calcification was classified as psammoma bodies, stromal calcification, or bone formation [13].

The presence of *psammoma bodies* is a diagnostic characteristic of papillary thyroid carcinoma. It is defined as spherical calcified foci with

concentric laminations, and is usually located within stromal stalks of tumor papillae, and is distinct from intrafollicular inspissated colloid [17]. In addition, in our experience, it is occasionally observed inside *stromal calcifications*. *Bone formation* was regarded as positive only when both bone matrix and osteocytes were identifiable [13].

All calcific masses that did not meet the criteria of psammoma bodies or bone formation were categorized as stromal calcifications, including psammomatoid calcifications, which are characterized by a spherical shape lacking laminations or by an irregular shape with laminations.

Histological features include psammoma bodies, stroma calcification, bone formation, age, sex, tumor diameter, extrathyroid invasion, pT, widespread lymph node metastases, histological lymph node metastases, stage grouping, and surgical margin are risk factors for recurrence. These include psammoma bodies, age, extrathyroid invasion, pT, common lymph node metastases, histological lymph node metastases, stage grouping, and surgical margin were identified as significant risk factors in the one-way analysis. Subsequent multivariate analysis showed that old age (Z60 years) and the presence of common lymph node metastases were independent predictors of recurrence; there was no such association for psammoma bodies [13].

Mechanisms of pathological biomineralization

In general, pathological biomineralization or calcification divides into dystrophic and metastatic [18].

In dystrophic biomineralization, calcium salts are deposited in areas of necrosis. Deposits of calcium salts are found in dead tissues or tissues in a state of deep dystrophy. The leading cause of dystrophic biomineralization is the physicochemical change of tissues, which ensures the absorption of calcium salts from the blood and tissue fluid [18]. During dystrophic biomineralization, crystalline minerals formed, consisting of calcium phosphate in apatite, similar to bone hydroxyapatite. This process consists of initiation and propagation and develops both in cells and extracellular space. Outside the cell, the initiation phase occurs in vesicles with a membrane about 20 nm in diameter. Calcite concentrate in these vesicles due to its affinity for acidic phospholipids, and phosphates accumulate due to membrane-bound phosphatases. Initiation of intracellular mineralization occurs in the mitochondria of dead or dying cells that get calcium [19]. Crystals form during the propagation phase. It depends on the concentration

of calcium and phosphorus in the extracellular space and the presence of mineral inhibitors, collagen, and other proteins. Osteopontin is involved in bone mineralization and dystrophic biomineralization. Collagen accelerates crystal formation [20].

Metastatic biomineralization occurs in normal tissues in hypercalcemia caused by: hyperparathyroidism, hypothyroidism, vitamin D intoxication, systemic sarcoidosis, Addison's disease, idiopathic hypercalcemia [21].

The *molecular basis* of PB formation, stromal calcification, and thyroid ossification is unknown. For example, the thyroid cell carcinoma cell line 8505C can produce BMP-1 and BMP-2 [22]. BMP-1 or procollagen-C-peptidase is a metalloproteinase enzyme; other bone-forming proteins, such as BMP 2-7, are proteins similar to β -transforming growth factor (TGF- β) [23]. BMP-1 can convert protein precursors, such as laminin-5, procollagen, growth and differentiation factors 8 and 11, and TGF- β 1, into their active forms, which play diverse roles in cell adhesion and regulation mineralization. BMP-1 can also activate two other proteins of the BMP family: BMP-2 and BMP-4, destroying their antagonist, chordin [23]. Among other bone-forming proteins under the conditions of thyroid pathology, BMP-9 was studied [24], which is one of the most osteogenic subtypes of bone-forming proteins. It was found that under the conditions of ossification in BMD, the expression of BMP-9 significantly increased. It is not observed in the absence of signs of tissue mineralization [25]. The association of PT formation with BMP-11 expression and osteopontin has also been reported. These proteins are produced by macrophages [26].

In addition to proteins of the BMP family, TGF- β , and osteopontin, there are reports of participation in the biomineralization processes of differentiated malignant thyroid tumors of molecules such as Runx2, CD44v6, and osteocalcin [27].

The signs of pathological biomineralization can be an essential differential diagnostic criterion for thyroid tumors both in ultrasound and histopathological examination. This is especially true for patients with calcification of the lymph nodes of the neck.

Pathologists should pay special attention to psammoma bodies that are unrelated to tumor pathology. This appearance may be a sign of latent thyroid cancer (microcarcinoma) or thyroid cancer metastasis from the opposite lobe of the gland.

2. Materials and methods

Research design

The study group included 123 patients with differentiated thyroid cancer (DTC) (papillary and follicular type of tumor), who at the stage of clinical examination showed no signs of regional metastasis to the cervical lymph nodes (cT1-4N0M0). There were 108 women (87.8%) and 15 men (12.2%). Surgical treatment was performed using the contrast-visual method of thyroidectomy with central and bilateral selective cervical lymph dissection (levels VI; II-A; III; IV).

Based on the cytological conclusion of the punctate tumor, papillary cancer was diagnosed in 105 (85.4%) patients with follicular cancer – in 18 (14.6%). The prevalence of cancer was determined by the clinical and morphological classification of thyroid tumors by the TNM system. The second stage of the tumor process was found in 88 (71.5%) patients, the first – in 27 (22%), the third – in 8 (6.5%). The diagnosis of thyroid cancer, its histological form, location, tumor size, extent, and regional metastasis was confirmed by special methods (computed tomography and ultrasound of the thyroid gland and all areas of the neck with Doppler, puncture, and subsequent cytological examination).

Kocher standard operative access with an extension of incisions in both directions in the McVay modification was used. The skin and muscle flap were widely separated from the underlying tissues (the lower limit was the jugular notch, the upper – the hyoid bone, the lateral – the lateral edge of the sternoclavicular-mammary muscle. Then the anterior surface of the thyroid gland was exposed only in the tumor area, maximum preservation of lymphatic pathways for better visualization of the regional lymphatic collector. In the tumor tissue with a syringe was injected 1% solution of toluidine blue.

The mean volume of 1% toluidine blue injected into the tumor was 1.2 ml (minimum 0.9 ml, maximum 1.6 ml).

After contrast was injected into the tumor, the puncture site was pressed with a gauze ball for one minute to prevent it from leaking and staining adjacent tissues. Then, for 2-3 minutes, a light massage of the thyroid gland was performed to improve the outflow of contrast through the lymphatic system and, accordingly, better visualization of the regional lymph collector (Figure 1).

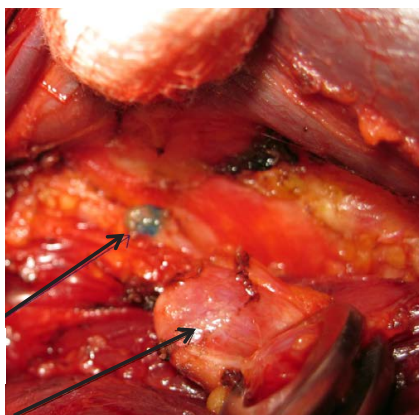


Figure 1. Lymph nodes in thyroid cancer. The sentinel lymph node is colored toluidine blue – indicated by one of the arrows. Another arrow indicates an inattentive lymph node with metastasis

Surgical treatment performs in two stages. Thyroidectomy is committed in a block with a central lymphatic collector of the neck (level IV). This block included paratracheal, prelaryngeal, and parathyroid tissue of the neck in the first stage. Particular attention was paid to allocating all lymph nodes (sentinel and non-sentinel). Observance of zonation of remote lymph nodes was an obligatory condition. Urgent intraoperative histological examination of thyroid tumors and distant sentinel lymph nodes was performed.

Cervical lymph dissection was performed with removal of fiber II-A; III; IV levels of the neck, with mandatory revision of the VB level

of VB in the second stage of the operation. Isolation of all lymph nodes (stained and unstained) and urgent histological examination of stained lymph nodes was also performed.

The Ethics Committee

The study was approved by the ethics committee of the Medical Institute of Sumy State University (Proceedings 3/4, 01 April 2021).

Ultrasound

We used Toshiba Applio MX with a linear multifrequency sensor 6-12 MHz (Tokyo, Japan) for ultrasound imagining at the Sumy Regional Oncological Hospital (Sumy, Ukraine).

Detection of Pathological Biominerals

The mineral component of macroscopic calcifications was separated from soft tissues by heat treatment at 200 °C for 1 hour. This contributed to the destruction of the organic compounds of the calcification and the removal of water residues while maintaining the structure of the crystallite. Pathological biomineral formations with a diameter of less than 0.05 cm were

detected by histology and scanning electron microscopy from histological sections of tumor tissue [28].

Histology

Thyroid tumor tissue material fixed in neutral (buffered) 10% formaldehyde solution for 24 hours – histological blocks prepared after dehydration and paraffin saturation. Serial sections with a thickness of 4 μm prepare using a rotary microtome Shandon Finesse 325 (Thermo Scientific). After dewaxing and dehydration (xylene and ethanol), histological sections were stained with hematoxylin and eosin. All photos were captured with a digital visualization system based on a Zeiss Primo Star microscope with a Zeiss Axiocam ERc 5s digital camera and software package “Zen 2.0” (Carl Zeiss, Jena, Germany).

Histochemistry

To detect calcium deposition, we used von Kossa staining. Histological dehydrated sections of tumor tissue were treated with 5% aqueous solution of silver nitrate under the direct light of a 60 W lamp for 60 minutes followed by washing in sodium thiosulfate (5% aqueous solution). Nuclei were counterstained with an aqueous solution of nuclear fast red for 5 minutes (1:1000) [29].

Scanning Electron Microscopy (SEM) with EDX

Histological sections with a thickness of 7 μm were mounted on a spectrally pure graphite base. Sections were preheated at 60 °C for 30 minutes, deparaffinized and dehydrated with xylene and ethanol. We used an SEO-SEM Inspect S50-B (SEO, Sumy, Ukraine) scanning microscope with an AZtecOne energy dispersion spectrometer with an X-MaxN20 detector (Oxford Instruments plc, Abingdon, UK). EDX spectra were analyzed with standard software of the microanalysis system [30].

X-Ray Diffraction

A DRON-4-07 diffractometer (Petrel, St. Petersburg, Russia) was used for X-ray diffraction of biominerals. Data were analyzed with the software package DIFWIN-1 (Etalon-PTC, Moscow, Russia). The phase composition identification was performed with the JCPDS database (Joint Committee on Powder Diffraction Standards) [29; 30].

Transmission Electron Microscopy

A PEM-125K microscope (SEMI, Sumy, Ukraine) was used for transmission electron microscopy (TEM) with electron diffraction (ED). The

powder of mineralized tissue was sonicated in distilled water with the UZDN-A sonicator (SELMI, Sumy, Ukraine). The specific power of the installation was 15–20 W/cm² at a frequency of 22 kHz. The suspension (a few drops) was applied to the vertically upward ultrasonic emitter UZDN-A and sprayed for 2–3 seconds at optimal power. The sprayed aerosol was attached to a thin carbon film (10–20 nm) mounted on a copper mesh of the sample holder. ED pictures and microphotographs were captured at voltage $U(\text{acceleration}) = 90 \text{ kV}$ [11].

Statistics

The normality of data distribution was checked by a Shapiro–Wilk test. Student’s t-test was applied for analysis of data with a normal distribution. Mann–Whitney’s U test was applied for nonparametric datasets. The results were considered statistically significant with a probability of more than 95% ($p < 0.05$). Statistical analysis was performed in Microsoft Office Excel 2016 with the addon AtteStat (version 12.0.5).

3. Results

Macroscopic examination of TC shows the tumor nodule presence (often in the form of a scar), with whitish-pink color. Tumor lymphatic nodules’ sizes ranged from 0.8 to 4.0 cm (Figure 2A). The nodule tissue has a dense consistence, often with small solid gray-white foci (Figure 2B). On a cut the surface of the tumor has often a small-grained relief, foci of cystic (cystic-like) changes are observed. Solid inclusion of tumor tissue crumbled during mechanical affecting, they were cut with a distinctive crunch.

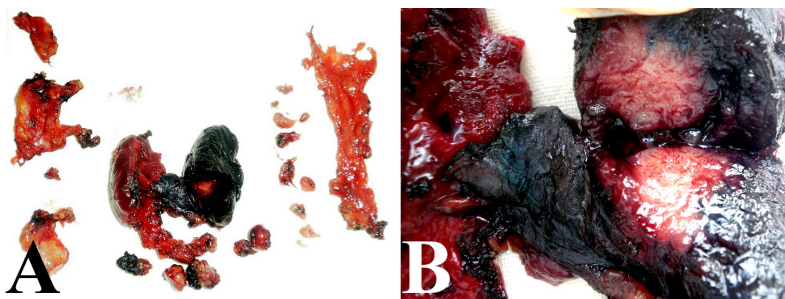


Figure 2. Removed thyroid gland with lymph nodes and fat. A – general view, B – the primary tumor of the thyroid gland in the form of pink-gray tissue inside the gland tissue

After applying this contrast method, we found SLN in 120 (97.6%) patients. The lymph node metastases ranged from 2 to 12 (mean 4.2). In 91 (75.8%) patients, the lymph nodes were located in the central collector of the neck on the side of the primary tumor (central, ipsilateral SLN). We found SLN metastases in 33 (27.5%) of 120 patients based on intraoperative studies. In 4 patients, the metastatic process confirms based on the final histological examination (Figure 3), and during the intraoperative assessment of these lymph nodes, metastases were not detected.

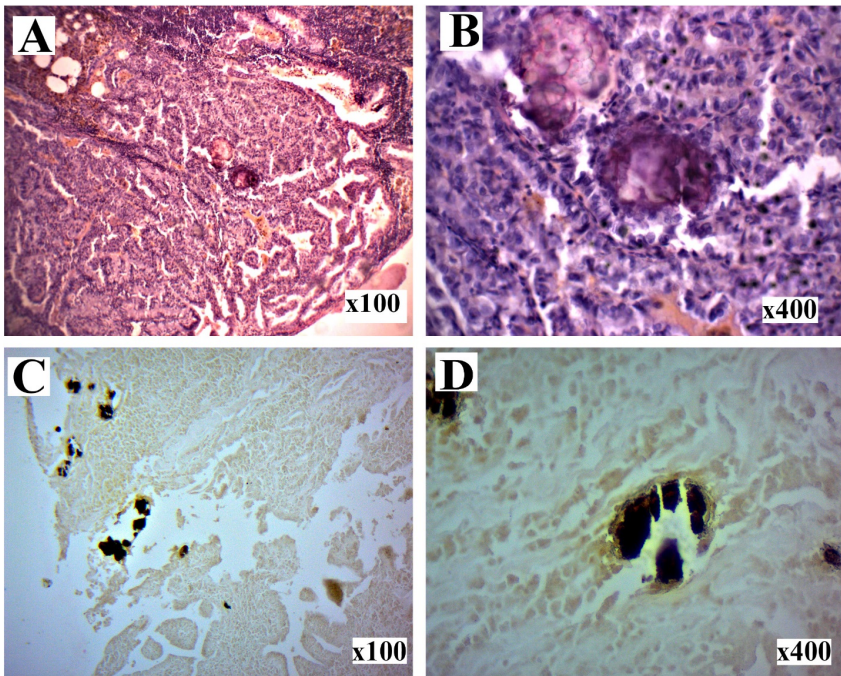


Figure 3. Histological and histochemical examination of the lymph node with thyroid metastasis. Hematoxylin and eosin staining. A – metastatic tissue with papillary and follicular structure signs in the lymph node, B – formation of mineralized psammoma cells in metastatic tissue. C, D – staining psammoma bodies by the method of von Koss. The magnification is indicated in the lower right corner of the photomicrograph

We show that thyroid metastases are more common in subcapsular areas of the lymph node. In some cases, the metastatic tissue completely displaces the lymphoid tissue, filling the entire node space. We found 19 cases of calcifications in metastatic lymph nodes (51,4%). All cases of pathological biomineralization of lymph nodes correspond to metastatic papillary thyroid cancer. The main form of calcification is psammoma bodies (Figure 3B). Psammoma bodies were found among the tumor tissue or in the subcapsular area solitary, without tumor cells.

The staining of calcified lymph node tissue by the von Koss method reflects the presence of calcium phosphate salts. Psammous bodies and their fragments in the tumor tissue turn black and dark brown (Figure 3C). The layers' boundaries are apparent in the PT, and the different color saturation between the nucleus and the shell of the formation is observed (Figure 3D).

Thus, we detected metastases in SLN in 37 patients (30.8%). Nineteen patients had signs of pathological biomineralization in the lymph nodes. In all cases of calcification, we diagnosed papillary thyroid cancer. Thus, the negative predictive value of intraoperative examination of sentinel lymph nodes was 89.2% (33 of 37 cases). We establish any diagnostic differences in determining the positive status of SLN during an intraoperative and final histological examination. Thus, the positive predictive value was 100%. Based on the final histological examination, the metastatic level of non-guarded lymph nodes strictly correlates with this indicator in SLN. Therefore, the false-negative rate in our study is zero. In 13 (35.1%) patients, the metastatic process presents only in sentinel lymph nodes.

Scanning Electron Microscopy with EDX

This work studied 19 samples of pathological mineral deposits of lymph nodes of papillary thyroid cancer in terms of their elemental and structural-phase composition. If any specific structural or concentration features of the calcification were found, each specimen's clinical history and etiology could be readily ascertained.

According to the SEM data, the mineralized material of the deposits consisted of particles of various sizes of arbitrary shape with signs of a brittle fracture along the edges. Of undoubted interest is the determination of the predominant crystallographic orientation of the mineral relative to the gland's surface. In some cases, we see layering (linear structure) of mineral deposits (Figure 4A, B). SEM detected that calcifications were

represented as round particles with a fragile structure and different sizes. It was confirmed by the presence of fragments of chimeric configuration. At high-power magnification, the fracture surfaces had a porous structure. Nanocrystalline structures of spherical and needle shapes were found on the surface of calcifications.

The point EDX analysis was carried out to reveal the major composition of PBs by subjecting representative PBs for this type of analysis (Figure 4, lower row). It showed that the major elements of PB were P and Ca. The amount of calcium in psammoma bodies was much higher than in hydroxyapatite with significant difference in Ca:P ratio 1.67 for HA.

X-ray diffraction

Blurry and overlapping lines characterize X-ray diffraction patterns of calcifications. In most cases, the phase composition of the samples is

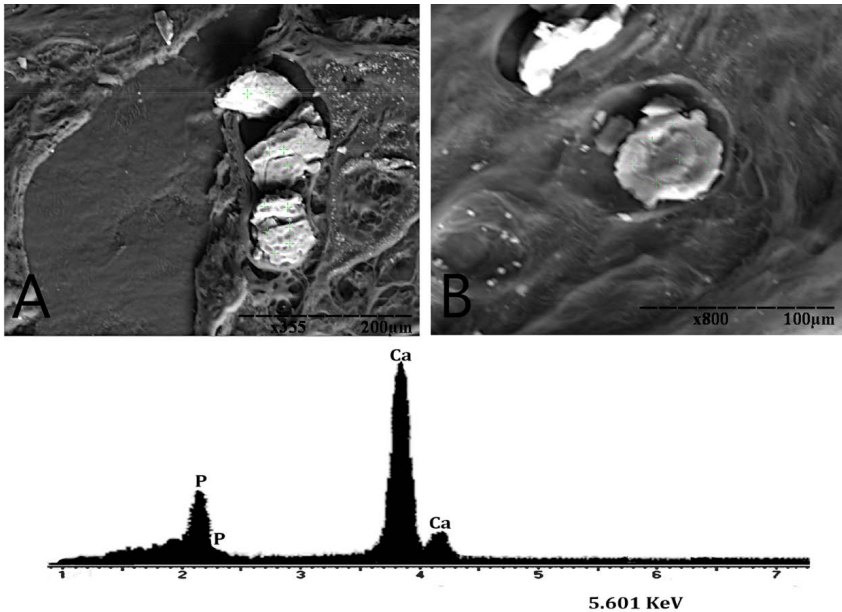


Figure 4. Scanning Electron Microscopy (SEM) with energy-dispersive X-ray spectroscopy (EDX), analysis points are marked by green crosses; EDX spectra of lymphatic node calcifications

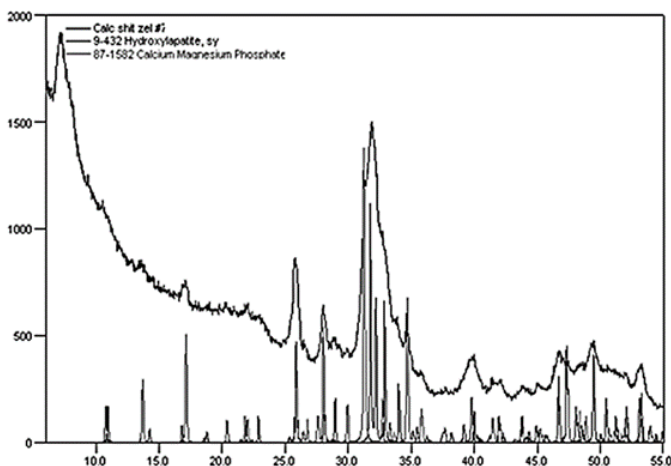


Figure 5. Typical diffraction pattern of annealed biomineral component of a calcified lymph node in thyroid cancer

represented exclusively by apatite with varying degrees of crystallinity. In some cases (Figure 5), we found weak signs of another phase – β TCMP (tricalcium magnesium phosphate). For most samples, the Scherrer crystallite size estimate in the expected direction to the (0 0 2) plane gives a spread of values from 14 to 30 nm [33].

According to the data of complex studies (X-ray and electron diffraction), pathological thyroid calcifications are nanocrystalline defective calcium apatite with a significant proportion of carbonate substitutions in the lattice (in the position of phosphate ions). We didn't find visible signs of other crystalline phases. We did not find stable relationships between X-ray diffraction data and this type of pathology. The phase-crystal composition corresponds to other malignant pathology of the thyroid gland.

Transmission electronic microscopy

According to TEM data, crystalline particles of calcifications, as a rule, are polydisperse (different in size), and the spread of their sizes can be pretty significant (Figure 6). Almost every sample has its specific features regarding the morphology and size of the crystals and the ED pattern formed by them. Based on this, under the condition of adequate preparation of the

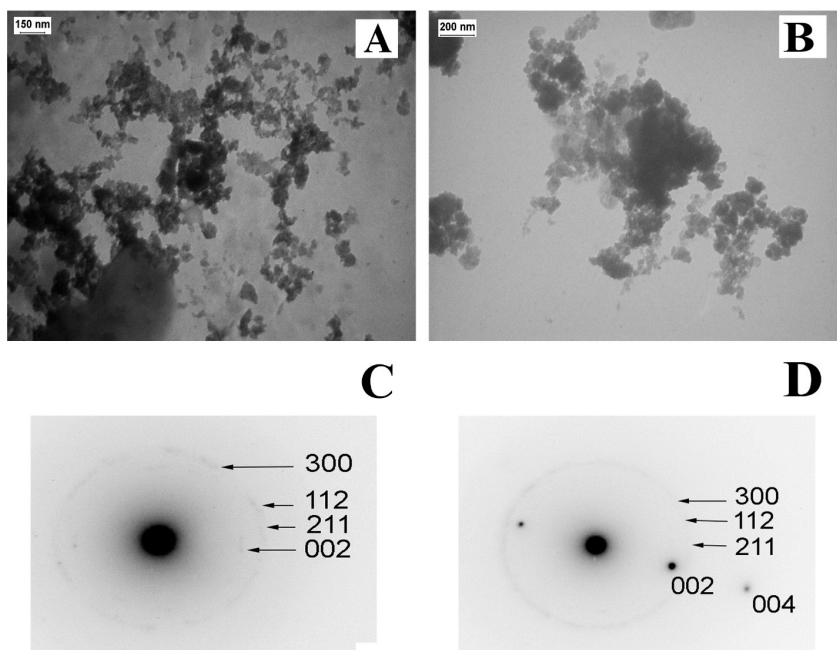


**Figure 6. TEM of lymph node calcified samples.
(A–B) TEM images of nanocrystals; (C–D) ED image**

initial material with mechanical isolation of localized micro-calcifications, it seems possible to study the dependence of individual TEM and ED data on the location of the deposit. As expected, this should be the subject of further research.

Therefore, in our studies, pathological calcifications of lymph node samples in thyroid cancer revealed the presence of apatite crystalline phase or phases (most likely hydroxyapatite ($\text{Ca}_5(\text{PO}_4)_3\text{OH}$, JCPDS № 9-432) according to X-ray diffraction phase analysis.

Describing the diffraction patterns shown in Figure 4, we found that in the structure of calcifications of the studied samples, in contrast to the standard, there is a shift of the diffraction pattern towards phosphorus and magnesium, i.e., the structure of calcification in addition to hydroxyapatite contains β -tricalcium magnesium phosphate.

4. Discussion

The calcification process is one of the clinical and morphological features of the manifestation of thyroid tumors. At the same time, it is not fully understood and needs to be studied in detail [13]. In the case of malignant tumors, pathological biomineralization begins at the earliest stages. This process is due to the partial death of malignant tumor cells, detritus which is the basis for constructing microcalcifications [10; 14; 17]. Therefore, this phenomenon can be used for the early diagnosis of some malignant neoplasms of the thyroid gland.

Today, some routine and high-tech non-invasive diagnostic methods are used, such as ultrasound, computed tomography (CT), magnetic resonance imaging (MRI), intravascular ultrasound (IVUS), optical coherence tomography (OCT), positron tomography (ECT), positron tomography (PET). Technological advances make it possible to diagnose smaller and smaller objects. However, these diagnostic methods have different resolutions.

Earlier, when comparing the ultrasound and histological examination results, we found that calcifications less than 200 μm are not detected by ultrasound methods [31].

At the same time, CT scans detect pathological deposits from 1000 microns. IVUS allows you to diagnose calcifications with 100-200 microns resolution. And the most high-tech and informative method is OCT, the resolution of which is 10-20 microns. A study by Shioi and co-authors showed that some stones might be X-ray negative [32]. It depends on the composition of pathological biominerals.

5. Conclusions

Our study demonstrated the significance of PBM in lymph nodes as a diagnostic symptom of papillary thyroid cancer patients. The presence and extent of PBM in the lymph nodes should be considered a metastasis of papillary thyroid cancer.

Our study found that the main component of pathological biomineral deposits is calcium phosphate compounds. The Ca / P ratio corresponds to the characteristic features of hydroxyapatite. A significant proportion of β -tricalcium magnesium phosphate was also detected in some cases. The specific plate structure and the known phase and crystal-chemical

composition of psammoma bodies can be the point of application of searches for their early detection using the latest diagnostic methods with high resolution.

The study of the structure, physicochemical, phase composition of lymph node calcifications, and visualization features is promising given the possible practical application for early diagnosis of metastases of papillary thyroid cancer.

The specific plate structure and the known phase and crystal-chemical composition of psammoma bodies can be the point of application of searches for their early detection using the latest diagnostic methods with high resolution.

6. Acknowledgments

This research has been performed with the financial support of grants of the Ministry of Education and Science of Ukraine No. 0112U100471 “Condition of mineralized tissues using new composites with Ag + and Cu₂ + nanoparticles”.

Conflicts of Interest: The authors declare no conflict of interest.

References:

1. Kang J.B., Kim E.Y., Park Y.L., Park C.H. & Yun J.S. (2017). A comparison of postoperative pain after conventional open thyroidectomy and single-incision, gasless, endoscopic transaxillary thyroidectomy: a single institute prospective study. *Ann Surg Treat Res*, 92:9–14.
2. Sharma C. (2016). An analysis of trends of incidence and cytohistological correlation of papillary carcinoma of the thyroid gland with evaluation of discordant cases. *J Cytol*, 33:192–198.
3. Rowe C.W., Murray K., Woods A., Gupta S., Smith R., Wynne K. (2016). Management of metastatic thyroid cancer in pregnancy: risk and uncertainty. *Endocrinol Diabetes Metab Case Rep*, p:16–0071.
4. Kulbakin D., Chekalkin T., Muhamedov M., Choyzonov E., Kang J.H., Kang S.B. & Gunther V. (2016). Sparing Surgery for the Successful Treatment of Thyroid Papillary Carcinoma Invading the Trachea: A Case Report. *Case Rep Oncol*, 9:772–780.
5. Sydorenko O.M., Sydorenko M.O., Tymoshev M.P. (2018) [The epidemiology of thyroid cancer in the twentieth and early twenty-first century in Ukraine and Zaporizhzhia region]. *Current issues in pharmacy and medicine: science and practice*, 11(3):322–325. DOI: <https://doi.org/10.14739/2409-2932.2018.3.144485> (in Ukrainian)
6. Fedorenko Z.P., Mykhailovych Yu.Y., Hulak L.O., Horoch E.L., Ryzhov Ayu, Sumkina O.V. et al. (2021) [Cancer in Ukraine, 2019–2020]. *Biuletен natsional-*

noho kantser-reiestru Ukrainy, 22:64–65. Available at: http://ncru.inf.ua/publications/BULL_22/PDF/BULL_22.pdf

7. Shirley L.A., Jones N.B. & Phay J.E. (2017). The Role of Central Neck Lymph Node Dissection in the Management of Papillary Thyroid Cancer. *Front Oncol*, 7:122. DOI: <https://doi.org/10.3389/fonc.2017.00122>

8. Kravets O.V., Kurochkin A.V., Moskalenko Yu.V., Moskalenko R.A. & Kuzmenko V.V. (2021). Detection of sentinel lymph nodes in patients with thyroid cancer with the use of toluidine blue. *Eastern Ukrainian Medical Journal*, 9(4), 401–409. DOI: [https://doi.org/10.21272/eumj.2021;9\(4\):401-409](https://doi.org/10.21272/eumj.2021;9(4):401-409)

9. Guerlain J., Perie S., Lefevre M., Perez J., Vandermeersch S., Jouanneau C., Huguet L., Frochot V., Letavernier E., Weil R., Rouziere S., Bazin D., Daudon M. & Haymann J.P. (2019). Localization and characterization of thyroid microcalcifications: A histopathological study. *PLoS One*, 14(10):e0224138. DOI: <https://doi.org/10.1371/journal.pone.0224138>

10. Das D.K. (2009). Psammoma body: a product of dystrophic calcification or of a biologically active process that aims at limiting the growth and spread of tumor? *Diagn Cytopathol*, 37(7):534–541. DOI: <https://doi.org/10.1002/dc.21081>

11. Chyzhma R., Pidubnyi A., Stepanenko A., Danilchenko S. & Moskalenko R. Morphology of Nanocrystalline Calcifications of Ovarian Tumors (2021). *IEEE 11th International Conference Nanomaterials: Applications & Properties (NAP)*, pp. 1–4. DOI: <https://doi.org/10.1109/NAP51885.2021.9568609>

12. Seiberling K.A., Dutra J.C., Grant T., et al. (2004). Role of intrathyroidal calcifications detected on ultrasound as a marker of malignancy. *Laryngoscope*, 114:1753–1757.

13. Bai Y., Zhou G., Nakamura M., Ozaki T., Mori I., Taniguchi E., Miyauchi A., Ito Y. & Kakudo K. (2009). Survival impact of psammoma body, stromal calcification, and bone formation in papillary thyroid carcinoma. *Mod Pathol*, 22(7):887–094. DOI: <https://doi.org/10.1038/modpathol.2009.38>

14. Moskalenko R., Romaniuk A., Riezniak A. & Kurochkin A. (2016). Papillary thyroid cancer with biomineralization: clinical and morphological features. *Pathologia*, 1(36):29–36. DOI: <https://doi.org/10.14739/2310-1237.2016.1.71182>

15. Ferreira L.B., Gimba E., Vinagre J., Sobrinho-Simões M. & Soares P. (2020). Molecular Aspects of Thyroid Calcification. *Int J Mol Sci.*, 19;21(20):7718. DOI: <https://doi.org/10.3390/ijms21207718>

16. Yin L., Zhang W., Bai W. & Ning, B. (2020). Relationship Between Morphologic Characteristics of Ultrasonic Calcification in Thyroid Nodules and Thyroid Carcinoma. *Ultrasound Med. Biol*, 46, 20–25.

17. Johannessen JV & Sobrinho-Simoes M. (1980). The origin and significance of thyroid psammoma bodies. *Lab Invest*, 43:287–296.

18. Giachelli C.M. (1999). Ectopic calcification: gathering hard facts about soft tissue mineralization. *Am J Pathol*, 154(3):671–675.

19. Pacifici M. (2018). Acquired and congenital forms of heterotopic ossification: new pathogenic insights and therapeutic opportunities. *Current opinion in pharmacology*, 40: 51–58.

20. Tunio G.M., Hirota S., Nomura S. et al. (1998). Possible relation of osteopontin to development of psammoma bodies in human papillary thyroid cancer. *Arch Pathol Lab Med*, 122:1087–1090.

21. Chiew Ken Seng & Cheng Yong Fatt. (2020). The silver lining: pleural calcification in an end-stage renal disease patient with tertiary hyperparathyroidism. *The journal of the Royal College of Physicians of Edinburgh*, 50.2: 164–165.

22. Sung, H., Ferlay, J., Siegel, R. L., Laversanne, M., Soerjomataram, I., Jemal, A., & Bray, F. (2021). Global cancer statistics 2020: GLOBOCAN estimates of incidence and mortality worldwide for 36 cancers in 185 countries. *CA: a cancer journal for clinicians*, 71(3), 209–249.

23. Ge G. & Greenspan D.S. (2006) BMP1 controls TGFbeta1 activation via cleavage of latent TGFbeta-binding protein. *J Cell Biol*, 175:111–120.

24. Hatakeyama S., Gao Y.N., Ohara-Nemoto Y, et al (1997). Expression of bone morphogenetic proteins of human neoplastic epithelial cells. *Biochem Mol Biol Intern*, 42:497–505.

25. Hopkins D.R., Keles S. & Greenspan D.S. (2007). The bone morphogenetic protein 1 / Tolloid-like metalloproteinases. *Matrix Biol*, 26:508–523.

26. Denhardt D., Giachelli C. & Rittling R. (2001). Role of osteopontin in cellular signaling and toxicant injury. *Annu. Rev. Pharmacol. Toxicol*, V.41:723–749.

27. Herring G.M. (1999). The organic matrix of bone. *The Biochemistry and Physiology of bone.*, G.H. Bourne, Ed. V. 1, pp. 127–189, Academic Press, New York.

28. Moskalenko, R., Danilchenko, S., Piddubnyi, A., Chorna, I., Kolomiets, O. & Romaniuk, A. (2020). Morphological and crystal chemical characteristics of gallbladder biomineralization. *Acta Fac. Med. Naissensis*, 327, 139–148.

29. Chyzhma R., Piddubnyi A., Danilchenko S., Kravtsova O. & Moskalenko R. (2021). Potential Role of Hydroxyapatite Nanocrystalline for Early Diagnostics of Ovarian Cancer. *Diagnostics*, 11, 1741. DOI: <https://doi.org/10.3390/diagnostics11101741>

30. Radomychelski, I., Piddubnyi, A., Danilchenko, S., Maksymova, O., Moskalenko, Y., & Moskalenko, R. (2021). Morphological and Crystal-Chemical Features of Macro- and Microcalcifications of Human Aorta. *Microscopy and Microanalysis*, 27(6), 1539–1546. DOI: <https://doi.org/10.1017/S1431927621012721>

31. Rieznik A.V., Hapchenko A.V., Hapchenko V.V., Starkiv M.P. & Moskalenko R.A. (2015) [Ultrazvukove ekho biomineralizatsii shchypodibnoi zalozy]. *J. Clin. Exp. Med. Res.*, 3(2):188–98. (in Ukrainian)

32. Shioi A. & Ikari Y. (2018). Plaque calcification during atherosclerosis progression and regression. *J Atheroscler Thromb*, 25:294–303. DOI: <https://doi.org/10.5551/jat.RV17020>

33. Klug H.P. & Alexander L.E. (1974). *X-Ray Diffraction Procedures: For Polycrystalline and Amorphous Materials*. New York: Wiley.